The 2010 IEEE/RSJ International Conference on
Intelligent Robots and Systems
October 18-22, 2010, Taipei, Taiwan

An Extended Normalized Cuts Method for Real-Time Planar Feature Extraction from Noisy Range Images

GuruPrasad M. Hegde, Cang Ye, Senior Member IEEE, Gary Anderson, Senior Member IEEE

Abstract— **This paper presents a new method for extracting planar features from noisy range data. The method encodes the local geometric information (surface normals) and global spatial information (coordinates) of 3D data points into an Enhanced Range Image (ERI) which is then clustered into a number of homogeneous groups, called Super Pixels (SPs). The Normalized Cuts (NC) method is employed to the graph built on the SPs and groups the SPs into planar segments. The ERI coding enhances object surfaces and edges while its sensitivity to surface normals is suppressed by the NC measure that takes into account the spatial information of SPs in computing the edge weights of the graph. A binary matrix is constructed to represent the spatial and similarity relationships among the planar segments. We then employ a search algorithm on this matrix to merge homogenous planar segments. The proposed approach is compared with a representative plane segmentation method in various indoor environments and the results demonstrate the efficacy of the proposed method. In this paper, rang data are captured from a 3D imaging sensor—the Swissranger SR-3000.**

I. Introduction

One of the research goals of mobile robotics is to enable autonomous navigation of a mobile robot in indoor environments (e.g., offices, industrial spaces, household environments). The navigational task includes navigating a robot from floor to floor in a building. To achieve this capability, a robot first needs to perceive its operating environment in 3D and then process the 3D data for obstacle detection/recognition and perform obstacle avoidance/ negotiation. Laser Detection and Ranging (LADAR) [1] and stereovision systems [2] have been extensively used in the existing research. A LADAR system usually has a low range data throughput and is good for 3D map-building with a stationary platform. The state-of-the-art 3D Velodyne LADAR [3] overcomes this problem by using 64 laser sensors. However, it is too big and bulky for an indoor robot. A stereovision system is not suitable for 3D dense map-building because the stereo matching can not return complete depth data in its field of view [4]. Recent advancements in range sensing technology have led to a new class of 3D imaging sensors, know as Flash LADARs [5], [6], [7]. A Flash LADAR illuminates the entire scene by a modulated light source. Each cell of the sensor can determine the time-of-flight of the modulated signal and thus the depth information of the detected object. In this work we use one such Flash LADAR—the Swissranger SR-3000 [6] to acquire 3D range data. We use the SR-3000 because we are targeting autonomous navigation of a small mobile robot in indoor environments. The SR-3000 is well suited to our case. It is small in size (50×48×65 mm^3), has a high data throughput—176×144 (25344) data points per frame and up to 50 frames per second. In addition, the SR-3000 works well in featureless environments which is advantageous over a stereovision system. However, the SR-3000's sensing technology is nascent and its range data has relatively large measurement errors (much bigger than that of a LADAR [8]) due to its random noise and susceptibility to environmental factors (e.g., surface reflectivity). Previous research efforts [9], [10] have demonstrated that a proper calibration process may reduce the errors in the SR-3000's range data to certain extent. However, it cannot eliminate the measurement errors induced by random noise. The noise-induced range error imposes challenges on segmenting range data into its geometric constituents—an essential step for range data understanding. Since an indoor environment typically consists of structures formed by flat surfaces such as walls, corridors, and staircases, we restrict this work to planar feature extraction of 3D range data.

Researchers have attempted to extract planar surfaces of range data either in 3D data space $\Re^3$ [11], [12], [13], [14], [15], [16] or from a range image [17], [18], [19]. The performances of some of the well known methods are compared in [20], according to which the USF method [20] may produce relatively low number of under segmented regions. The USF method is a region-growing method. It first computes the normal vector and a so-called interiorness measure for each point. They are determined by fitting a plane to its surrounding points within a $N \times N$ window. The point's normal vector and the interiorness are and the fitted plane's normal and the fitting error, respectively. To start the segmentation process, a point with the smallest interiorness value is selected as a seed for region growing. Four-connected points join the region if: (1) the angle between normal of point and normal of the region is within a threshold; (2) perpendicular distance between point and the region's plane is less than a threshold; and (3) distance between point and the four-connected neighbor in the region is below a pre-specified threshold. The region grows recursively until no point can further join. A new seed point is again selected based on its interiorness measure and the process repeats. Another common segmentation approach in $\Re^3$ is to sequentially extract planar surfaces by a robust

Manuscript received March 10, 2010. This work was supported in part by the National Science Foundation and NASA.

The authors are with the Department of Applied Science, University of Arkansas at Little Rock, Little Rock, AR 72204, USA. (Phone: 501-683-7284; Fax: 501-569-8020; E-mail: cxye@ualr.edu)

least-square estimator [11], [16]. The method determines and labels inliers of a planar surface by fitting a parametric plane model to range data and examining the fitting error. A limitation of this type of plane-fitting based methods is that the fitting error (i.e., an averaged squared error of the fit) is not sufficiently accurate to distinguish inliers from outliers and thus may result in misclassification.

Extraction of planar surfaces from a range image is usually performed on an edge-/surface-enhanced range image that encodes surface normals [17], [18]. This type of methods tends to locate edges (intersections of planar surfaces) accurately but the performance may be greatly affected by noises of range data that induce variations in surface normals.

In this paper, we use surface normal and depth information to enhance a range image. The scheme of image enhancement will be described in section III. Figure 1 illustrates a range image enhancement by the ERI scheme. In the ERI (Fig. 1c) the contrast between objects' surfaces and thus the objects' edges are enhanced. However, the surfaces are corrupted. The corruption (shown as surface roughness) is caused by large variations in surface normals induced by range noises. The corruption may greatly deteriorate the efficiency of the existing local feature based segmentation methods [11], [16], [17]. This demands a new segmentation method that uses both local and global criteria in segmenting the range data.

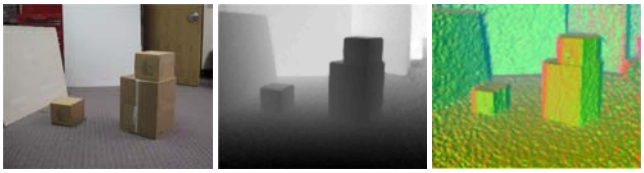

(a) (b) (c)

Fig.1 The range image and ERI: (a) Actual scene, (b) Range images acquired by the SR-3000, (c) ERI of (b).

In the literature of intensity image segmentation, recent algorithms [21], [22], [23] [24] based on spectral graph theory partition an image using intra-segment similarity (local information) and inter-segment dissimilarity (global information). It has been shown in [22] that the Normalized Cuts (NC) clustering method performs better than other spectral graph partitioning methods, such as the averaged cuts [23] and minimum cuts [24] methods, and produces globally optimal clusters. In this work, we extend the NC method to range image segmentation.

We will briefly introduce the NC method in section II and extend the NC method to range data segmentation in section III. Section IV presents the experimental results and comparison of our proposed method with the USF method; and the paper is concluded in Section V.

II. The Normalized Cuts Method

A. Image Segmentation as a Graph Partitioning Problem

Image segmentation can be modeled as a graph partitioning problem. An image is represented as a weighted undirected graph $G=(V,E)$ wherein each pixel is considered as a node V_i. An edge $E_{i,j}$ is then formed between a pair of nodes V_i and V_j. The weight for each edge is calculated as a function of similarity between each pair of nodes. In partitioning an image into various disjoint sets of pixels or segments $V_1,V_2,V_3,...,V_m$, the goal is to maximize the similarity of nodes in a set and minimize the similarity across different sets. With the NC algorithm, the optimal bipartition of a graph into two sub-graphs A and B is the one that minimizes the *Ncuts* value given by:

$$Ncut(A,B)=\frac{cut(A,B)}{assoc(A,V)}+\frac{cut(A,B)}{assoc(B,V)}, \quad (1)$$

where $cut(A,B)=\sum_{(u\in A,v\in B)} w(u,v)$ is the dissimilarity between A and B, and $w(u,v)$ is the weight calculated as a function of the similarity between nodes u and v. $assoc(A,V)$ is the total connection from nodes in A to all nodes in V, while $assoc(B,V)$ is the total connection from nodes in B to all nodes in V. From (1) we can see that a high similarity among nodes in A and a low similarity across different sets A and B can be maintained by the minimization process. Given a partition of nodes that separates a graph V into two sets A and B, let x be an $N=|V|$ dimensional indicator vector, $x_i=1$ if the i^{th} node is in A and -1, otherwise. Let $d_i=\sum_j w_{i,j}$ be the total connection from the i^{th} node to all other nodes. With the above definition, $Ncut(A,B)$ in (1) can be calculated. According to [21], if x is relaxed to take on continuous values, the optimal partitions can be obtained by splitting the graph using the Eigen vector corresponding to the second smallest Eigen value of the system:

$$(D-W)y=\lambda Dy, \quad (2)$$

where $D=diag(d_1,d_2,...,d_n)$, $d_i=\sum_j w_{i,j}$, $W=[w_{i,j}]$.

B. Grouping Algorithm

The grouping of pixels in an image $\boldsymbol{I}$ consist of the following steps:

a) Consider image $\boldsymbol{I}$ as an undirected graph $G=(V,E)$ and construct a similarity matrix W. As stated before, each element of W is the weight of edge $w_{i,j}$ and is calculated by

$$w_{i,j}=e^{-\frac{\|F(i)-F(j)\|_2^2}{\sigma_F}}\times e^{-\frac{\|X(i)-X(j)\|_2^2}{\sigma_Z}} \quad (3)$$

if $\|X(i)-X(j)\|_2\le r$ pixels; or $w_{i,j}=0$ otherwise. Here $X(p)$ (p stands for i or j) is the spatial location of nodes p, and $F(p)$ is the brightness (color information) of pixel p. $\|\bullet\|_2$ denotes the L^2-norm of a vector. This means that $w_{i,j}=0$ for a pair of nodes V_i and V_j if they

are more than r pixels apart. In other words, equation (3) computes each weight by taking into account the global information—distance between the two pixels. The heuristic behind this treatment is that two distant pixels are not likely belonged to a segment even if they have similar brightness.

b) Solve (2) for the Eigenvectors with the smallest Eigen values.
c) Use the Eigen vector with the second smallest Eigen value to bipartition the image by finding the splitting points such that its *Ncut* value is minimized.
d) Recursively re-partition the segments (go to step a)
e) Exit if *Ncut* value for every segment is over some specified threshold.

III. Proposed Method

In this work we adopt the method in [18] and represent a set of range data as a tri-band color image where each pixel's RGB values represent the x, y components of the surface normal $\vec{N}_p = [n_x, n_y, n_z]$ and the depth information (Y value) of the corresponding point in $\Re^3$. We use the following mapping for color coding:

$$\begin{cases} R = k_1 \cos^{-1} n_x \\ G = k_2 \cos^{-1} n_y \\ B = k_3 Y \end{cases}, \qquad (4)$$

where k_1, k_2 and k_3 are positive constants that scale the pixels' RGB values and map them into the range [0, 255]. It should be noted that: (1) the use of x and y components is sufficient to represent the surface normal since $n_z = \sqrt{1 - n_x^2 - n_y^2}$; (2) the row and column indices and the blue component (i.e., the Y value) of the tri-band image pixel fully determines the 3D coordinates of the corresponding data point in $\Re^3$. This means that the scheme encodes a 3D point's local geometric information (surface normal) and global information (location) into a pixel in the color image.

We call this RGB image an Enhanced Range Image (ERI) as it enhances the edges and surfaces of objects in the range image. As demonstrated in Fig. 1, the ERI conversion assigns different colors to the intersecting surfaces and makes the roof-edges distinctive. With this image enhancement, we can segment the range data by applying the NC method to the ERI. Since we use a color image, $F(i)$ in (3) is the norm of the color vector of the i^{th} node. The first and second terms in (3) represent the weight contributions of the color difference and spatial distance between the i^{th} and j^{th} nodes, representatively. The physical meaning of (3) is that: Two nodes are more likely in the same segment if they are spatially close and have similar surface normals.

A direct implementation of the NC method to an ERI is computationally expensive as the number of pixels is huge. In [25] this problem is alleviated by down-sampling the input image to a reasonable size. However, the weight computation is still costly. We resolve this computational bottleneck by: (1) clustering a set of nearby homogeneous pixels of an ERI into a group, called Super-Pixels (SPs); (2) constructing a graph that takes each SP as a node; and (3) applying the NC method to the graph. The spatial location and color of each SP are computed as the centroid and mean color value of its ERI pixels. In our method, a node of the graph corresponds to a region rather than a single ERI pixel. This reduces the graph's node number and thus the computational cost of the NC method. Our method is less sensitive to noise because: (1) the mean color computation of a SP smoothes the noise of the range data in the SP; and (2) the NC method takes both color and spatial information in clustering the SPs. The proposed method is described in the following subsections.

A. L*u*v Color Space Representation of ERI

In this work we use the Mean-Shift (MS) algorithm [26] to cluster an ERI into a number of SPs. Since the MS code [27] that we use only accepts L*u*v images, we convert an ERI from RGB to L*u*v color space. It is apparent that the ERI of an inclined plane has varying color due to the change in depth values (i.e., blue band). As a consequence, the MS clustering may result in over-segmentation. This is demonstrated in Fig. 2 where the MS algorithm is applied to a computer generated noise-free planar surface (Fig. 2a) and results in a number of SPs (Fig. 2d) rather than a single SP. Therefore, it becomes necessary to merge planar SPs. (A planar SP is one whose data points form a plane in $\Re^3$.) In this work the merger is a 2-stage process: (1) classify homogeneous SPs into a larger segment by the NC method; and (2) merge neighboring planar segments if the angle between their normals is small enough.

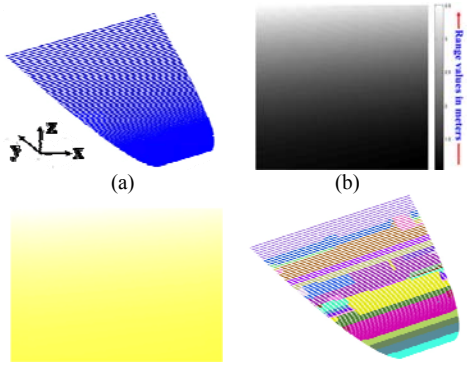

Fig. 2 MS segmentation of a simulated plane: (a) Simulated point-cloud, (b) Range image, (c) ERI of (b), (d) Segmentation results of the MS algorithm on (c).

B. Classification of Planar Segments

We first need to classify a segment as planar or non-planar. Here, a segment can be a SP or a region containing a number of SPs. A Least-Square Plane (LSP) is fitted to the data points of the segment, and the normal $\vec{N} = [n_x, n_y, n_z]$ and the Plane Fit Error (PFE) Δ is computed by the Singular Value Decomposition method [28]. A segment with a

sufficiently small Δ, i.e., $\Delta<\delta$, is labeled as a planar segment. The angle between planar segments i and j is computed by

$$\theta_{i,j} = \cos^{-1}(\vec{N}_i \bullet \vec{N}_j). \quad (5)$$

They are considered as parallel if $\theta_{i,j}$ is sufficiently small, i.e., $\theta_{i,j}<\varepsilon$.

C. Graph Construction and Partitioning

We construct a graph $G=(V,E)$ by treating each planar SP as a node. The edge weight, which is a measure of similarity between two nodes V_i and V_j, is calculated by

$$w_{i,j} = e^{-\frac{\|F(i)-F(j)\|_2^2}{\sigma_F}} \begin{cases} e^{-\frac{d_{i,j}}{\sigma_D}} & \text{if } V_i \text{ and } V_j \text{ are neighbors} \\ 0 & \text{otherwise} \end{cases} \quad (6)$$

where σ_F and σ_D are positive constants, $F(p)$ is the L*u*v color vector of node p for $p=i, j$, and $d_{i,j}$ is the Euclidean distance between the LSPs of SPs i and j (i.e., nodes i and j). If $\theta_{i,j}<\varepsilon$ is satisfied, then $d_{i,j}$ is the distance from the centroid of the data in SP i to the LSP of the data in SP j. Otherwise, $d_{i,j}=0$. Two SPs are considered as neighbors if they have at least two neighboring pixels in the ERI space. The weight computation in (6) takes into account the statistics of 3D data points. This may result in better segmentation results (as exemplified in IV).

We then apply the NC algorithm to the graph and cluster the SPs into a set of segments $S=\{s_1, s_2, \cdots, s_N\}$.

D. Labeling and Merging of Planar Segments

In this step, the segments in S are labeled as planar and non-planar according to III. *B*. Two neighboring planar segments i and j are further merged if $\theta_{i,j} \le \varepsilon$ and $d_{i,j}$ is less than a threshold τ.

In summary, the proposed plane extraction method is as follows:

a) Construct the ERI from the range data and apply the MS algorithm to obtain a number of SPs.
b) Obtain planar SP_i; for $i=1,\cdots,m$ from the resulted SPs according to III.B.
c) Construct a graph G on SP_i; for $i=1,\cdots,m$ and compute the similarity matrix $\boldsymbol{W}$ of order $n \times n$ by (6).
d) Apply the NC algorithm to graph G with $\boldsymbol{W}$ as the input and obtain N segments, s_i for i=1,...,N, each of which contains a number of SPs. Each segment r in s_i is further classified to form a set of planar segments $P=\{p_1, p_2, ..., p_t\}$; $t \le N$.
e) Construct a binary matrix $K=\{k_{i,j}|_{i=1,...,t;\, j=1,...,t}\}$ to record the neighborhood relationship among segments in P, where

$$k_{i,j} = \begin{cases} 1 \text{ if } p_i \text{ and } p_j \text{ are neighbors and } \theta_{i,j} \le \varepsilon, d_{i,j} \le \tau \\ 0 \text{ otherwise} \end{cases} \quad (7)$$

It is noted that a segment is treated as its own neighbor. Therefore, $k_{i,i}=1$.

f) In the final step, the entire planar surfaces are extracted by merging those segments whose k values equal zero. This is done by using the depth first search algorithm.

IV. Experimental Results

We have validated our method and compared it with the USF method with range data captured from the SR-3000 in a number of representative indoor environments. We implement the methods in Matlab 7.01 (R14) on a Sony Vaio–SZ220B laptop with a 1.83 GHz Intel Core Duo processor, 1GB RAM, and Windows XP OS. The rationale behind choosing the USF method is that it has a low rate of under-segmentation.

In all our experiments, a pre-specified segment number[1] N=75 is used for the NC method. For the results shown in this section, we represent an unlabelled segment in black and a labeled segment (a planar segment) with a random non-black color. The labeled segments are then overlaid on the ERI and Point-cloud data.

To demonstrate the function of the NC algorithm, we also run the proposed method without the NC component (i.e., by taking off steps c) and d) from the method). We refer this to Mean-Shift Dominated (MSD) segmentation method and the proposed method Extended Normalized Cuts (ENC) method. In this section we will compare them with the USF method. To measure each method's segmentation performance, we define a Segmentation Quality Index (SQI) given by

$$SQI = \frac{R-A}{A}, \quad (8)$$

where A is the actual number of planes (hand labeled in the experiments) and R is the resulting number of planes by the segmentation method. The sign of SQI indicates over-segmentation (positive sign) or under-segmentation (negative sign) and the magnitude of SQI represents the segmentation quality. A SQI value closer to 0 indicates a better segmentation result.

The first experiment is to segment the range data of a hallway (Fig. 3a). Figure 3b and Fig 3c display the range image and ERI, respectively. Figure 3d shows the 4 prominent planes in ERI found by hand labeling. After applying the MS algorithm to the ERI, we obtained 270 SPs as shown in Fig. 3e. The use of SPs causes a reduction of node number from 25344 to 270. As the edge number of a n-node graph is $n \times (n-1)/2$, the number of edge-weight computations is reduced from 321146496 to 36315, about 10^4 times smaller. This computational reduction will be referred to as Computational Reduction Factor (CRF) further on. The initial grouping of SPs using the NC method is shown in Fig. 3f. The extracted planar segments using the MSD and ENC methods are shown in Fig. 3g and Fig. 3h, respectively; while the result of the USF method is depicted in Fig. 3i. The 3D point-cloud rendering of the results are shown in Fig. 3j, Fig. 3k and Fig. 3l, respectively.

[1] We have currently devised a recursive cut method that removes the need of a pre-specified N values. However, it is beyond the scope of the paper. In fact, the pre-specified value does not affect the final segmentation result as long as the value is big enough.

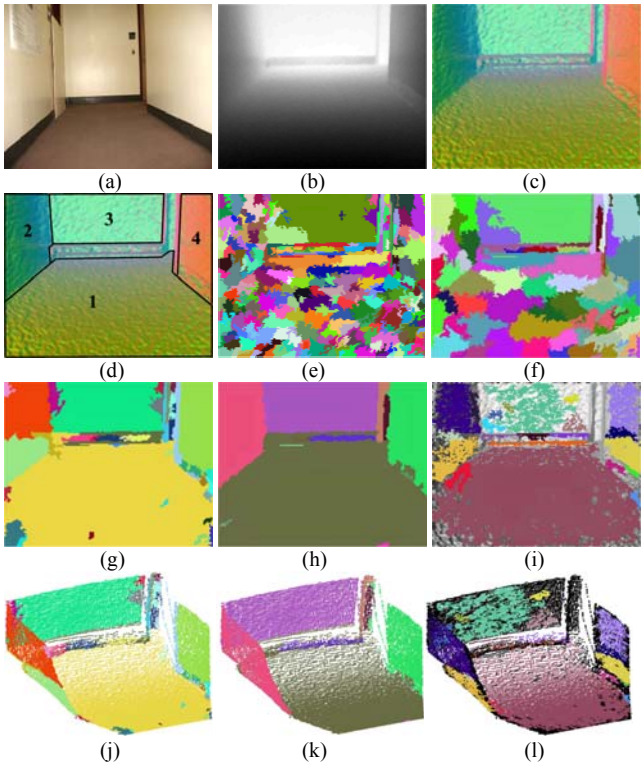

Fig. 3 Segmentation of the range data of a hallway: (a) Actual scene, (b) Range image, (c) ERI of (a), (d) ERI with prominent planes marked in black, (e) SPs of (c), (f) Results after applying the NC algorithm on (e), (g) Extracted planes using the MSD method, (h) Extracted planes using the ENC method, (i) Extracted planes by the USF method, (j) Point-cloud of (g), (k) Point-cloud of (h), (l) Point-cloud of (i).

From a qualitative perspective, the MSD results in fragmented walls (at planes labeled as 2 and 3) whereas the ENC method is able to extract the walls in their entirety. There are some misclassifications at the intersection of the front wall and floor in Fig. 3h. This is most likely due to the use of a small *N*. However it should be noted that their impact on navigating a robot may be ignored as they occurs at a faraway location from the robot. The USF method results in a huge number of unclassified pixels.

To quantify the segmentation result, we calculate the SQI of the MSD and ENC methods using (8). In this experiment A=4, R_{MSD}=28, R_{ENC}=8. Hence SQI_{MSD}=6 and SQI_{ENC}=1. This means that the ENC performs much better than the MSD. The SQI for the USF method is not calculated as the method resulted in a huge number of unclassified points.

The 2nd experiment was carried out to examine the method's performance on a scene with a stairway as shown in Fig. 4a. As we can see, the ENC method extracts most of the horizontal (tread) and vertical (riser) surfaces with less fragmentation than the other two methods. This is attested by the SQI. In this experiment A=10, R_{MSD}=59, R_{ENC} =14, resulting in SQI_{MSD}=4.9 and SQI_{ENC} =0.4. SQI_{ENC} is much closer to 0, indicating a better segmentation result.

The 3rd experiment was carried out to examine the method's performance in an environment with scattered obstacles. We tested this by placing two boxes and a trash can on the floor as shown in Fig. 5a. We can see from Fig. 5d that the MSD method results in under-segmentation on the top surface of each box. The boxes' top surfaces are merged with the floor surface. However, the ENC method extracts all of the surfaces with decent accuracy. This demonstrates that the ENC method can be used to extract the true extent of a floor and the surfaces of objects on the floor, an important capability for a robot to plan a collision free path. The quality of segmentation can further be verified by the SQI. In this case we have A=12, R_{MSD}=43, R_{ENC}=21, resulting in SQI_{MSD} =2.25 and SQI_{ENC}=0.41. Again, the ENC method outperforms the MSD method.

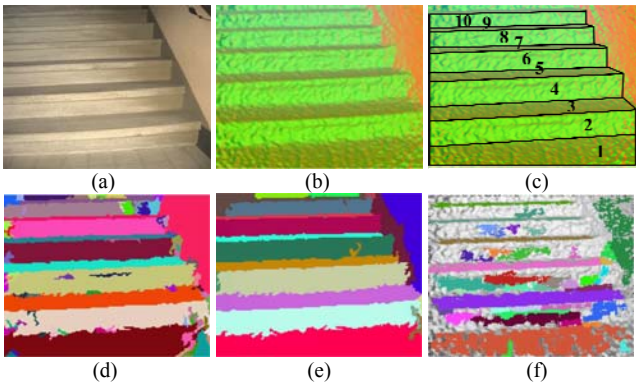

Fig. 4 Segmentation of the range data of a stairway: SPs=217, CRF=1.31×10^4: (a) Actual scene, (b) ERI of (a), (c) ERI with the marked prominent planes, (d) Extracted planes using the MSD method, (e) Extracted planes using the ENC method, (f) Extracted planes by the USF method.

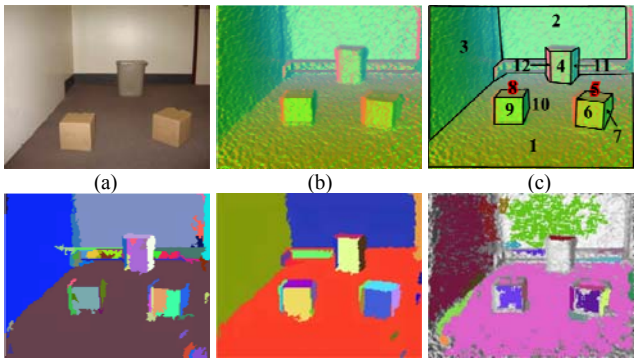

Fig. 5 Segmentation of the range data of a scene with scattered obstacles, SPs=277, CRF=8.4×10^3: (a) Actual scene, (b) ERI of (a), (c) ERI with the marked prominent planes, (d) Extracted planes using the MSD method, (e) Extracted planes using the ENC method, (f) Extracted planes by the USF method.

The runtimes of the above experiments are tabulated in Table I. It takes the ENC method ~10 seconds to segment a typical indoor scene. The ENC method's runtime in each case is only slightly (~10%) longer than that of the MSD due

TABLE I
RUNTIMES OF THE ENC AND MSD METHODS

Experiment	Scene	Runtime (seconds)	
		MSD	ENC
1	Hallway	8.48	9.37
2	Stairway	7.38	8.43
3	Scattered obstacles	9.23	10.42

to the additional NC computation. This indicates that our SP-based NC method is computational efficient. We expect that ENC method may achieve real-time performance after we implement it in C++.

We have performed additional experiments with various configurations of objects and the results are similar. This demonstrates that the inclusion of the NC method can substantially improve segmentation result. All of our experiments have also indicated that the proposed method performs much better than the USF method in the cases of noisy range data.

V. CONCLUSIONS

We have presented a new method that may reliably extract planar surfaces from noisy range data captured by the Swissranger SR-3000. The method extends the NC method to segment range data with relatively large random noise by using a new edge-weight function. The proposed method enhances object edges and surfaces by converting a range image into an ERI that encode the local geometric and global spatial information of the 3D data points. To reduce the computational cost, the MS method is used to preprocess the ERI and cluster the ERI into SPs. The plane-fitting statistics of these segments are used to label planar segments and merge homogeneous planar segments. From the experimental results, we find that the inclusion of the NC method results in a better segmentation result. This validates that the NC measure is able to suppress the effect of noise in range data. We have compared the performance of our method with the USF range image segmentation method. The results demonstrate that our method out-performs the USF method due to the use of global information. In all of our experiments, the proposed method achieves decent segmentation results even in a cluttered environment.

The method can be used for range image understanding, symbolic map-building, and navigation of a mobile robot.

REFERENCE

[1] C. Ye, "Navigating a mobile robot by a traversability field histogram," *IEEE Transactions on Systems, Man, and Cybernetics-Part B: Cybernetics*, vol. 37, no. 2, pp. 361-372, 2007.

[2] R. Turchetto and R. Manduchi, "Visual curb localization for autonomous navigation," in *Proc. IEEE/RSJ International Conference on Intelligent Robots and Systems*, 2003, pp. 1336-1342.

[3] http://www.velodyne.com/lidar/products/specifications.aspx

[4] C. Ye and M Bruch, "A visual odometry method based on the SwissRanger SR-4000," Proc. Unmanned Systems Technology XII Conference at the 2010 SPIE Defense, Security, and Sensing Symposium.

[5] R. Stettner, H. Bailey, and R. D. Richmond, "Eyesafe laser radar 3d imaging," in *Proc. SPIE*, vol. 4377 of *Laser Radar Technology and Applications*, September, 2001.

[6] T. Oggier, B. Büttgen,F. Lustenberger, "SwissRanger SR3000 and first experiences based on miniaturized 3D-TOF Cameras," *Swiss Center for Electronics and Microtechnology (CSEM) Technical Report,* 2005.

[7] S. B. Gktürk, H. Yalcin, and C. Bamji, "A time-of-flight depth sensor - system description, issues and solutions," in *Proc. IEEE Computer Society Conference on Computer Vision and Pattern Recognition Workshops*, 2004, pp. 35-35.

[8] C. Ye and J. Borenstein, "Characterization of a 2-D laser scanner for mobile robot obstacle negotiation," in *Proc. IEEE International Conference on Robotics and Automation*, 2002, pp. 2512-2518.

[9] S. A. Guomundsson, H. Aanaes, and R. Larsen, "Environmental effects on measurement uncertainties of time-of-flight cameras," in *Proc. International Symposium on Signals, Circuits and Systems,* 2007, pp. 1-4.

[10] K. Young Min, D. Chan, C. Theobalt, and S. Thrun, "Design and calibration of a multi-view TOF sensor fusion system," in *Proc. IEEE Computer Society Conference on Computer Vision and Pattern Recognition Workshops*, 2008, pp. 1-7.

[11] K.M Lee, P. Meer, and R.H. Park "Robust adaptive segmentation of range images," *IEEE Transactions on Pattern Analysis and Machine Intelligence*, vol.20, no.2, pp.200-205, 1998.

[12] R. Unnikrishnan and M. Hebert, "Robust extraction of multiple structures from non-uniformly sampled data," in *Proc. IEEE/RSJ International Conference on Intelligent Robots and Systems*, 2003, pp. 1322-1329.

[13] R. Triebel, W. Burgard, and F. Dellaert, "Using hierarchical EM to extract planes from 3d range scans," in *Proc. IEEE International Conference on Robotics and Automation*, 2005, pp. 4437-4442.

[14] V. Don and H. Maarten Uijt de, "Near real-time extraction of planar features from 3d flash-ladar video frames," in *Proc. SPIE, vol. 6977 of Optical Pattern Recognition*, pp. 69770N-69770N-12, 2008.

[15] I. Stamos and P. E. Allen, "3-d model construction using range and image data," in *Proc. IEEE International Conference on Computer Vision and Pattern Recognition*, 2000, pp. 531-536.

[16] L. Silva, O. Bellon, and P. Gotardo. "A global-to-local approach for robust range image segmentation," in *Proc. IEEE International Conference on Image processing*, 2002, pp. 773–776.

[17] R. L. Hoffman and A. K. Jain, "Segmentation and classification of range images," *IEEE Transactions on Pattern Analysis and Machine Intelligence*, vol. 9, no. 5, pp. 608–620, Sep. 1987.

[18] K. Pulli and M. Pietikainen, "Range image segmentation based on decomposition of surface normals," in *Proc. of the 8th Scandinavian Conference on Image Analysis*, 1993, pp. 893-899.

[19] S. Suganthan, S. A. Coleman, B. W. Scotney, "Single-step planar surface extraction from range images" Proc. 4th *IEEE International Symposium on 3D Data Processing, Visualization and Transmission*, 2008, pp. 363-372.

[20] A. Hoover, et al., "An experimental comparison of range image segmentation algorithms," *IEEE Transactions on Pattern Analysis and Machine Intelligence,* vol. 18, no. 7, pp. 673-689, 1996.

[21] J. Malik, S. Belongie, J. Shi, and T. Leung, "Textons, contours and regions: cue combination in image segmentation," in *Proc. International Conference on Computer Vision*, 1999, pp. 918-925.

[22] J. Shi and J. Malik, "Normalized cuts and image segmentation," *IEEE Transactions on Pattern Analysis and Machine Intelligence,* vol. 22, no. 8, pp. 888-905, 2000.

[23] S. Sarkar and P. Soundararajan, "Supervised learning of large perceptual organization: Graph spectral partitioning and learning automata," *IEEE Transactions on Pattern Analysis and Machine Intelligence*, vol. 22, no. 5, pp. 504–525, 2000.

[24] Z.-Y.Wu and R. Leahy, "An optimal graph theoretic approach to data clustering: theory and its application to image segmentation," *IEEE Transactions on Pattern Analysis and Machine Intelligence.*, vol. 15, no. 11, pp. 1101–1113, 1993.

[25] http://www.cis.upenn.edu/~jshi/software/: A matlab library for Normalised Cuts based image segmentation.

[26] W.Tao, H. Jin, and Y. Zhang "Color image segmentation based on mean shift and normalized cuts," *IEEE Transactions on Systems, Man, and Cybernatics,* part B, vol. 37, no. 5, pp. 1382-1389, 2007.

[27] http://coewww.rutgers.edu/riul/research/code/EDISON/index.html

[28] C. Ye, "A method for mobile robot obstacle negotiation," *International Journal of Intelligent Control and Systems,* vol. 10, no.3, pp. 188-200, 2005.